

# Utilizing Vegetation and Environmental New Micro Spacecraft (VEN $\mu$ S) Data to Estimate Live Fuel Moisture Content in Israel's Mediterranean Ecosystems

Avi Bar-Massada  and Achiad Sviri

**Abstract**—Increasing fire activity in Mediterranean ecosystems necessitates the development of new methods to quantify fire risk. Fire risk is strongly affected by live fuel moisture content (LFMC) in plants. Unfortunately, LFMC is time-consuming to measure *in-situ*. Remote sensing is a promising alternative to field sampling of LFMC, but existing approaches utilize sensors with high spatial resolution but infrequent revisit times, or frequent acquisition at coarse spatial grains. We developed and evaluated LFMC models for Israel's Mediterranean ecosystems using Vegetation and Environmental New Micro Spacecraft (VEN $\mu$ S), a satellite which was developed specifically for monitoring Mediterranean vegetation. We combined vegetation indices derived from VEN $\mu$ S with ancillary data to build statistical models of LFMC in six study sites located along a steep rainfall gradient. Out of the five vegetation indices we tested, only red-edge position was a significant predictor of LFMC, though its effect depended on tree cover. A model including red-edge position, tree cover, year-day, and slope-aspect explained 32.5% of the variation in LFMC. The moderate predictive power of this model was higher than expected given that VEN $\mu$ S does not have the shortwave infrared (SWIR) bands which are typically used to detect water content in plants. A comparison with six vegetation indices derived from Sentinel 2 data revealed that VEN $\mu$ S' data explained considerably more variation in LFMC, even though some Sentinel 2 VI's are based on SWIR bands. Our results suggest that VEN $\mu$ S data, combined with ancillary data, may provide a rough estimate of LFMC in Israel's Mediterranean regions and as such might be suitable for preliminary monitoring purposes.

**Index Terms**—Fire risk, live fuel moisture, Mediterranean, Sentinel 2, vegetation and environmental new micro spacecraft (VEN $\mu$ S).

## I. INTRODUCTION

MEDITERRANEAN ecosystems have been shaped by millennia of human activities, such as grazing, vegetation clearing, and fire [1]. These disturbances generated and

maintained highly heterogeneous landscapes, supporting high biodiversity and reduced wildfire risk [2]. In recent decades, though, socioecological changes around the Mediterranean basin have led to widespread expansion of woody vegetation [3]. This has altered the structure and composition of vegetated communities, and increased the amount and continuity of flammable vegetation, resulting in profound changes to biodiversity and ecosystem function, and increased fire risk [4]. On average, there are 1000 forest fires in the Mediterranean region in Israel every year [5]. In 2017 alone, the extent of burnt areas reached 4100 ha. Future climate projections predict an increase in the magnitude of extreme weather events in the region, which will be manifested by extended periods of severe drought [6], which can exacerbate the fire problem in the eastern Mediterranean region. To reduce the severity of the fire problem in eastern Mediterranean ecosystems, multiple avenues of action are needed, starting with continuous monitoring of vegetation cover and biophysical conditions in order to identify areas at risk of fire initiation and spread. These areas, in turn, can be modified by active management practices [7] such as fuel treatments based on livestock grazing or mechanical clearing [8]. Three types of variables can serve as predictors of fire risk [9]–[11]: Probability for fire ignition; the amount and type of vegetated fuel which is related to the dominant vegetative formations; and the biophysical condition of these fuels, specifically live fuel moisture content (LFMC). LFMC is a measure of plant dryness which is directly related to its combustibility, and consequently to its ability to ignite and support fire spread. In annuals, fresh foliage can reach LFMC level as high as 300%, whereas mature foliage which is comparable in structure to perennial foliage has LFMC levels around 100%, foliage of plants entering dormancy has LFMC around 50%, and completely cured vegetation which is comparable to dead fuel has LFMC below 30% [12]. There are strong empirical and experimental relationships between LFMC and fire ignition, spread, and to a lesser degree fire behavior. Hence, the ability to monitor changes at LFMC across large areas is crucial for predicting the risk of fire initiation and spread. LFMC affects the likelihood of fire ignition and spread (e.g., [13]), and fuel moisture content, which includes both dead (DFMC) and live (LFMC) components is a crucial component in many fire behavior models and fire-danger ranking systems

Manuscript received December 2, 2019; revised April 12, 2020 and June 2, 2020; accepted June 8, 2020. Date of publication June 11, 2020; date of current version June 22, 2020. This work was supported by the Israel Ministry of Science and Technology under Grant 3-14722. (Corresponding author: Avi Bar-Massada.)

Avi Bar-Massada is with the University of Haifa at Oranim, Kiryat Tivon 36006, Israel (e-mail: avi-b@sci.haifa.ac.il).

Achiad Sviri is with the Department of Evolutionary and Environmental Biology, University of Haifa, Haifa 3498838, Israel (e-mail: achiads@gmail.com).

This article has supplementary downloadable material available at <http://ieeexplore.ieee.org>, provided by the authors.

Digital Object Identifier 10.1109/JSTARS.2020.3001677

[14]–[16]. While DFMC can be readily estimated from meteorological data, LFMC is more difficult to estimate because it reflects specific adaptations of plants to drought and depends on site-specific conditions. Furthermore, LFMC varies with plant phenology, and has distinctive seasonal patterns. Nevertheless, previous studies have successfully linked LFMC with shrubland fires in California [17], [18], Catalonia [19], New South Wales [20], and Victoria, Australia [21]; and there are strong relationships between LFMC and burned area [22]–[25]. Specifically, LFMC levels below a threshold of  $\sim 70\%$  are associated with a sharp increase in burned area in California Mediterranean ecosystems [23], and the drop of LFMC below this level may signal severe fire risk.

LFMC can be readily measured in the field. It is, however, time consuming and impractical to measure it across broad extents. Alternatively, remote sensing approaches are promising tools for monitoring LFMC across large areas. LFMC mapping is constrained by site- and species-specific characteristics that affect the spectral reflectance of plants [26]. Estimation of LFMC from remotely sensed data is based on two approaches. Physical model-based approaches rely on physical models to estimate plant water content based on plant structure. Empirical approaches, in contrast, relate field-measured LFMC to satellite vegetation indices (VI; typically, those that include data on near infrared (NIR) and shortwave infrared (SWIR) reflectance, as water absorbs most of the radiation in these wavelengths). Many studies have used VI's as predictors of field-measured LFMC, with varying levels of success. For example, the normalized difference infrared index (NDII) is significantly correlated with LFMC in Mediterranean grasslands, shrublands, and woodlands [27], [28]. Another study [29] found that the normalized difference water index (NDWI) is significantly correlated with LFMC in chaparral vegetation in Mediterranean California. Beside VI's, coarse vegetation fractions from spectral mixture analysis (SMA; explained later) of high-resolution AVIRIS imagery are also strong predictors of LFMC in Mediterranean shrublands [28].

The success of both VI and SMA approaches in estimating LFMC in Mediterranean ecosystems in California and the western Mediterranean basin highlights their potential for the estimation of LFMC in eastern Mediterranean ecosystems. However, remote sensing estimates of LFMC are typically carried out at spatial scales that are much coarser (30–250 m) than the grain of heterogeneity of Israel's Mediterranean landscapes, where ecological information extraction is challenging because of high spatio-temporal variability in vegetation characteristics [30]. At the same time, fine-resolution RS platforms that can capture the fine-scale heterogeneity of these ecosystems typically lack the spectral bands needed for estimating LFMC, and have infrequent revisit times (precluding them from being effective monitoring tools). To address these limitations, we suggest the utilization of remotely sensed data from a new satellite-based sensor, Vegetation and Environmental New Micro Spacecraft (VEN $\mu$ S), which is jointly operated by the Israeli and French space agencies. With its high revisit time (every other day) and high spatial resolution (5–10 m, depending on data product), VEN $\mu$ S offers

TABLE I  
VEN $\mu$ S CAMERA CHARACTERISTICS

| Band | Quantity               | Central wavelength (nm) | Bandwidth (nm) |
|------|------------------------|-------------------------|----------------|
| 1    | Atmospheric correction | 423.9                   | 40             |
| 2    | Aerosol, clouds        | 446.9                   | 40             |
| 3    | Atmospheric correction | 491.9                   | 40             |
| 4    | Land                   | 555                     | 40             |
| 5    | Land                   | 619.7                   | 40             |
| 6    | DEM, image quality     | 619.5                   | 40             |
| 7    | Land                   | 666.2                   | 30             |
| 8    | Land                   | 702                     | 24             |
| 9    | Land                   | 741.1                   | 16             |
| 10   | Land                   | 782.2                   | 16             |
| 11   | Land                   | 861.1                   | 40             |
| 12   | Water vapor            | 908.7                   | 20             |

a compromise between the benefits of high resolution (but infrequent) aerial imagery, and moderate resolution (but frequent) satellite imagery. VEN $\mu$ S, therefore, may be a promising tool for monitoring LFMC in Mediterranean ecosystems. Hence the objective of this study was to evaluate the efficacy of VI's derived from VEN $\mu$ S data to estimate LFMC in Israel's Mediterranean ecosystems.

## II. METHODS

### A. VEN $\mu$ S Data

We obtained VEN $\mu$ S data from the official distribution site.<sup>1</sup> VEN $\mu$ S acquires images of Israel along three swaths (eastern, western, and southern) in a north-to-south flight path. The satellite has a circular, sun synchronous orbit at an altitude of 720 km, and its swath width is 27.5 km. Revisit time is two days, and overpass time is 10:30 in the morning. The Super Spectral Camera has a catadioptric objective, a focal plane assembly with narrow-band filters and four detector units with three separate CCD-Time Delay Integration arrays each [31]. VEN $\mu$ S collects spectral reflectance data in 12 spectral bands, ranging from 420 to 910 nm, with bandwidths ranging from 16 to 40 nm (Table I). Raw VEN $\mu$ S data undergo geometric calibration with same algorithm as Sentinel 2, and radiometric calibration using algorithms described in [32], and an additional processing stage includes the generation of a cloud mask. The field study sites in which we collected LFMC data are contained within six VEN $\mu$ S tiles (Fig. 1, Table II). We downloaded VEN $\mu$ S Level-2 products, which contain surface reflectance data at a

<sup>1</sup>Online. [Available]: <https://venus.bgu.ac.il/venus/>.

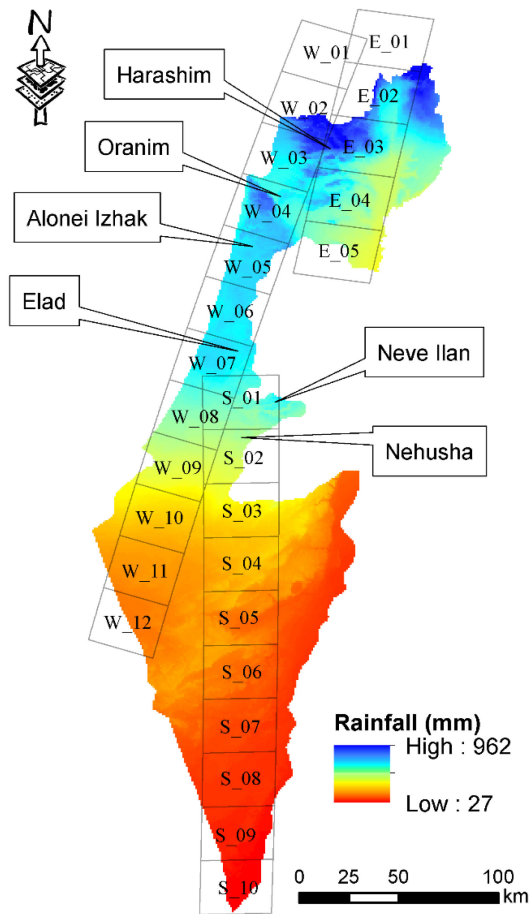


Fig. 1. Study site locations overlaid on the long-term (1980–2010) average precipitation map of Israel. VEN $\mu$ S tiles across three strips above Israel are depicted by rectangles, with tile names written inside each rectangle.

TABLE II  
VEN $\mu$ S VEGETATION INDICES USED IN THIS STUDY

| Name                              | Reflectance equation   | VEN $\mu$ S bands | Reference |
|-----------------------------------|--|-------------------|-----------|
| NDVI                              | $(\rho_{865}-\rho_{620})/(\rho_{865}+\rho_{620})$                        | 6, 11             | [33]      |
| Red edge 1 NDVI                   | $(\rho_{782}-\rho_{702})/(\rho_{782}+\rho_{702})$                        | 8, 10             | [34]      |
| Red edge 2 NDVI                   | $(\rho_{782}-\rho_{742})/(\rho_{782}+\rho_{742})$                        | 9, 10             | [34]      |
| Red edge Inflection point         | $702+40(((\rho_{667}+\rho_{782})/2)-\rho_{702})/(\rho_{742}-\rho_{702})$ | 7, 8, 9, 10       | [35]      |
| Canopy Water Content Index (CWCI) | $(\rho_{865}-\rho_{910})/(\rho_{865}+\rho_{910})$                        | 11, 12            | -         |

10-m spatial resolution which corresponds with our field data collection protocol (see below). At the time of data acquisition, level-2 data were only available at this resolution; however, starting from summer 2019, all VEN $\mu$ S level-2 products were reprocessed to 5-m spatial resolution, but the lack of fit with our field data precluded us from using these products in the

analysis. Overall, we downloaded and processed data from 24 VEN $\mu$ S images, in order to generate a suite of vegetation indices for each one of our field study sites.

Due to problems with boundary pixels in the W03 VEN $\mu$ S tile, which covers the northernmost study site, and partial obstruction by clouds in other tiles, our dataset contained VI values for 94 VEN $\mu$ S pixels (out of 120 for which we had field data). After data truncation to ensure normality (see below), we retained 82 pixels, based on which we fit the statistical models of LFMCI.

### B. Vegetation Indices

Satellite indices that are useful for estimating LFMCI typically include information from NIR and SWIR bands [26], [28]. Unfortunately, while VEN $\mu$ S has two NIR bands, it does not have SWIR bands; hence the estimation of LFMCI using VEN $\mu$ S was restricted to those vegetation indices that are based on reflectance values between 420 and 910 nm. We selected five VEN $\mu$ S vegetation indices that were expected to provide reasonable estimates of LFMCI (Table II; Fig. 2): Normalized difference vegetation index (NDVI); [33], Red-edge 1 NDVI [34]; Red-edge 2 NDVI [34]; Red-edge inflection point [35]; and Canopy water content index (CWCI). We identified the values of all vegetation indices and their corresponding field-based measures of LFMCI in multiple sampling dates (see next section), and utilized the time series of these values, together with ancillary variables, to build statistical models for LFMCI.

### C. Field Study

To measure LFMCI content in the field, we selected six field study sites which are located along Mediterranean Israel's precipitation gradient, from  $\sim 400$  to  $\sim 960$  mm/y (Table III; Fig. 1, Fig. S1). Measurement of LFMCI *in situ* was based on repeated field sampling in the six study sites. A full description of study site characteristics appears in Table S1. The sampling period coincided with the peak fire season (July to October), in 2018. Each field site was revisited four times, approximately at monthly intervals (Table III). Sampling dates were restricted to days that had less than 10% cloud cover, to facilitate comparison with satellite imagery. The first sampling date occurred more than three weeks after the last rainy day of the year, in order to avoid LFMCI values that are too high to support wildfire ignition and spread.

In each site, we allocated five circular study plots, and geolocated their centers using GPS. Individual plots were located in areas of homogeneous slope and aspect, and when possible, in areas that are surrounded by similarly structured vegetation (at least within 30-m radius) to ensure better correspondence between field and satellite estimators of LFMCI in cases of imperfect geolocation matching. To improve the generality of the estimated relationship between field-based LFMCI and its satellite-based estimation, in each site we allocated plots at different slope aspects (where possible). In each plot, we estimated the percent cover of all main life-forms (trees, shrubs, dwarf shrubs, and herbaceous vegetation, which are the main vegetation types in eastern Mediterranean landscapes, and form the spectral mixture which is present at pixel sizes larger than a few meters) using two perpendicular line-transects of 10-m



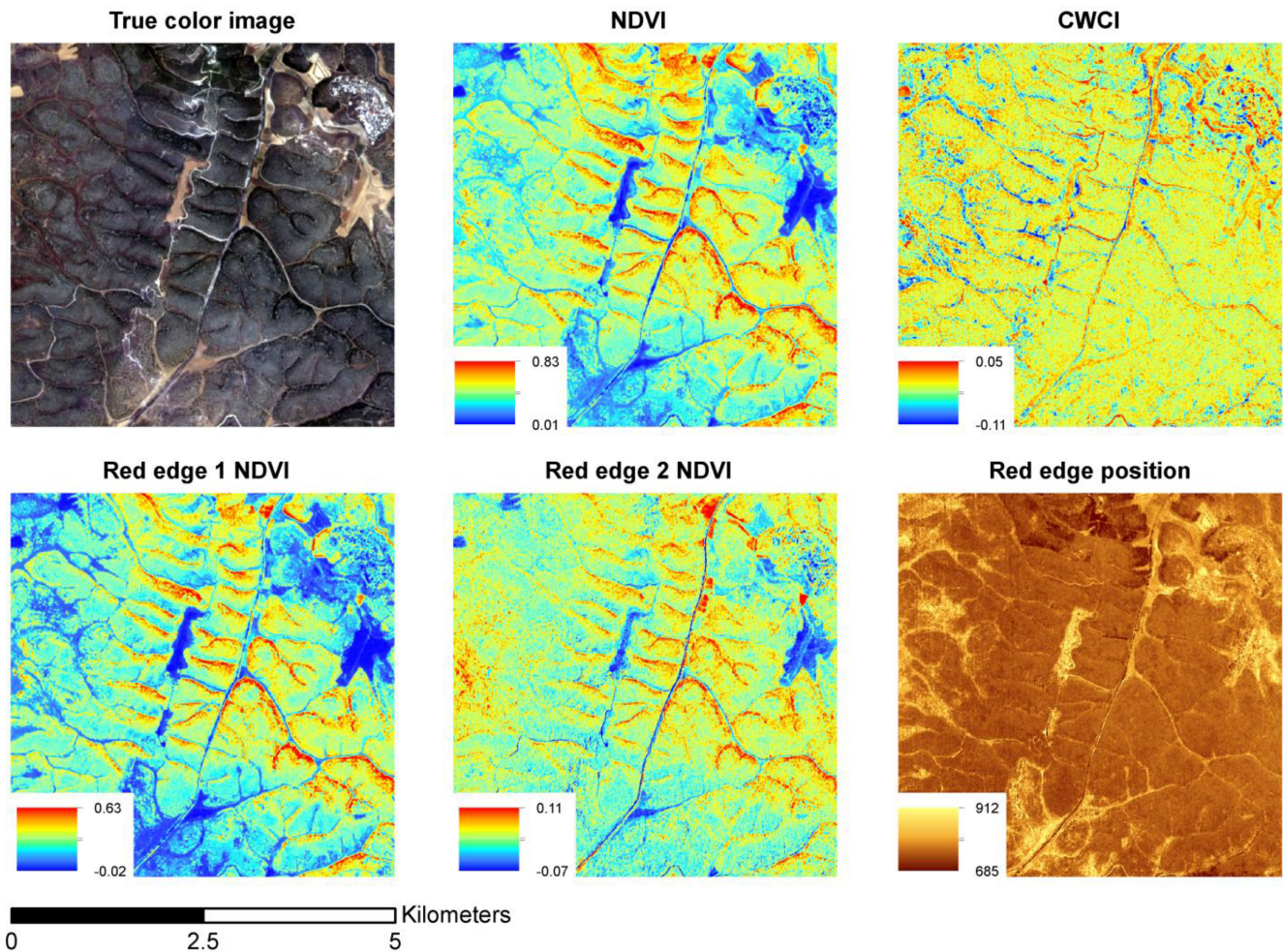


Fig. 2. True color composite of a VEN $\mu$ S image of the area around Nehusha field site, acquired on August 16th, 2018; and the five VI's used in this study.

TABLE III  
STUDY SITE CHARACTERISTICS AND INFORMATION ABOUT CORRESPONDING  
VEN $\mu$ S IMAGERY IN 2018

| Name<br>(Tile)           | Lat/ Long         | Mean<br>annual<br>rainfall<br>(mm) | Date 1 | Date 2 | Date 3 | Date 4 |
|--------------------------|-------------------|------------------------------------|--------|--------|--------|--------|
| Harashim<br>(W03)        | 32.955/<br>35.330 | 959                                | 27/6   | NA     | 1/9    | NA     |
| Oranim<br>(W04)          | 32.713/<br>35.107 | 597                                | 7/7    | 27/7   | 1/9    | NA     |
| Alonei<br>Izhak<br>(W05) | 32.035/<br>34.966 | 569                                | 11/7   | 6/8    | 11/9   | 13/10  |
| Elad<br>(W07)            | 31.810/<br>35.072 | 589                                | 9/7    | 10/8   | 11/9   | 13/10  |
| Neve Ilan<br>(S01)       | 32.513/<br>35.003 | 617                                | 9/7    | 6/8    | 11/9   | 13/10  |
| Nehusha<br>(S02)         | 31.644/<br>34.922 | 403                                | 19/7   | 16/8   | 13/9   | NA     |

length, intersecting at the center of the plot. We then collected 10 samples of leaves and small stems (3.2 mm or less, following [28]) at 1-m intervals along each 10-m transect. If several individual plants overlapped vertically in a sampling point, we collected data from the top-canopy individual because it was more likely to reflect radiation to the satellite sensor. Samples were weighted in the field to establish their wet weight ( $W_w$ ), placed in bags, and then transported back to the lab where they were oven-dried at 60 °C for 24 h, and reweighted to obtain dry weight ( $W_d$ ). We then calculated the LFCM for each sample using:  $LFCM = (W_w - W_d) / (W_d) \times 100$ . The LFCM values obtained from the analysis of 20 samples from each pair of perpendicular transects were averaged to yield a single LFCM value per plot, corresponding with a single VEN $\mu$ S pixel. This LFCM measure was then used, in conjunction with the data from the remote-sensing analysis of the corresponding pixel, to generate statistical models of LFCM (see next section). Overall, we collected and measured LFCM for 2400 field samples (20 samples per plot, five plots per site, six sites overall, multiplied by four sampling dates).

#### D. Comparison With Sentinel 2 Vegetation Indices

To contextualize the results obtained from VEN $\mu$ S data, we obtained and analyzed Sentinel 2 data for the same study sites and periods (Table S2). From these data, we generated six vegetation indices which either correspond with the VEN $\mu$ S VI's detailed above, or complement them by including spectral data from SWIR bands, which are known to contain useful information about plant moisture content, but are not present in VEN $\mu$ S data. The six Sentinel 2 VI's were: NDVI, Red-edge 1, Red-edge 2, Red-edge position 1, Normalized difference Infrared Index (NDII; also known as Normalized Different Moisture Index – NDMI), and Global Vegetation Moisture Index (GVMI). The formulae for these indices appear in Table S3.

#### E. Statistical Models of LFM C Based on VEN $\mu$ S and Ancillary Data

LFMC is likely to vary across sites and dates (due to variation in climatic conditions and site characteristics), and across slope aspects within sites (due to variation in solar radiation levels). Hence a statistical model for estimating LFM C should account for the temporal trend in LFM C, which is characterized by a monotonic decrease throughout the dry season in eastern Mediterranean ecosystems (Bar-Massada *et al.*, in preparation), and for differences in topographic conditions among sites. Furthermore, the fine-grained spatial heterogeneity of Mediterranean habitats means that even at 10-m grain, the ground area which corresponds with a given pixel may comprise multiple individual plants of different species, interspersed with open ground and rocks [36], [37]. Hence at this scale ecological information comprises the composition of life-forms; and consequently, the signal of vegetation indices at the pixel level comprises a spectral mixture of the reflectance of different plant life forms, together with soil and rock. Consequently, a statistical model that predicts LFM C from satellite data in eastern Mediterranean ecosystems should include information about the fractional cover of the main life-forms, especially trees, which comprise the dominant component in the canopy and reflect most of the radiation. To account for these issues, we developed models based on multiple linear regressions, with LFM C as the dependent variable, and a given vegetation index, the slope aspect (north, south, or flat; as three levels of a categorical variable), the sampling date (as Julian day), and the fractional cover of trees in the pixel as predictor variables. Given that the effect of a vegetation index on LFM C is expected to vary with tree cover, we also included in the models an interaction term between tree cover and vegetation index value.

While the model specification outlined above reflects the combination of most important predictors of LFM C known from the literature, we are aware that there might be other variables related to LFM C which we did not consider. We therefore complemented the multiple regression models with univariate models of LFM C as a function of any given VI, in which variation in conditions within and among sampling sites was accounted for without an explicit specification of predictor variables. We did this by fitting linear mixed effects models with LFM C as the dependent variable, a given VI as the fixed

effect, and plot identity nested within site identity as a random intercept effect. We fit these models using maximum-likelihood, and evaluated the significance of the fixed effect using a type-II Wald chi-square test.

Prior to model generation, and regardless of model type, we ensured that the dependent variable was normally distributed by truncating LFM C values above 100%. We evaluated normality using the Shapiro–Wilks test, and by visual inspection of normal-quantile plots. We found that prior to truncating LFM C to 100% or below, the response variable was not normally distributed (Shapiro–Wilks test,  $W = 0.9$ ,  $p < 0.001$ ), whereas after truncation it was normally distributed (Shapiro–Wilks test,  $W = 0.97$ ,  $p = 0.07$ ).

### III. RESULTS

#### A. LFM C Dynamics

LFMC values ranged from 37.53% to 97.14%, with a mean of 67.59%. On average across all sites (irrespective of the effects of other possible explanatory variables), LFM C decreased significantly by 0.16 ( $\pm 0.02$  S.E.) per day throughout the study period (linear mixed effects model with LFM C as the dependent variable, Julian day as the fixed effect, and sampling plot nested within site as a random intercept effect).

#### B. LFM C Models

Four of the five VI's we used in the analysis were moderately to highly correlated, which is expected given the partial overlap in the reflectance bands used in their calculation. Specifically, NDVI and Red-edge 1 NDVI were highly correlated ( $r = 0.94$ ), as were NDVI and Red-edge 2 NDVI ( $r = 0.84$ ). Both Red-edge NDVI indices were moderately correlated ( $r = 0.72$ ), whereas Red-edge position was only highly correlated with Red-edge 2 NDVI ( $r = 0.85$ ). Finally, CWCI had very low correlations with all other VI's, never exceeding  $r = 0.1$ .

Out of the five VEN $\mu$ S vegetation indices that we used as predictors of LFM C, only Red-edge position proved to be a significant predictor of LFM C in our multiple regression analysis (Fig. 3). A model that included Red-edge position, tree cover, the interaction of Red-edge position and tree cover, slope-aspect, and Julian day as predictors of LFM C was statistically significant ( $p < 0.001$ ) and explained 32.5% of the variation in LFM C across sampling sites and dates. According to this model, Julian day had a significant negative effect on LFM C ( $\beta = -0.12$  (S.E. 0.03),  $p = 0.001$ ), LFM C was significantly lower on both south-facing and north-facing slopes compared to flat areas ( $\beta = -12.01$  (S.E. 3.42),  $p = 0.0007$ ; and  $\beta = -11.7$  (S.E. 3.05),  $p = 0.0002$ , respectively). Both Red-edge position and tree cover had a significant positive effect on LFM C ( $\beta = 2.86$  (S.E. 1.07),  $p = 0.009$ ; and  $\beta = 4697$  (S.E. 1346),  $p = 0.0008$ , respectively), but the interaction between their effects was significantly negative ( $\beta = -6.51$  (S.E. 1.86),  $p = 0.0008$ ). This negative interaction implies that the effect of Red-edge position on LFM C varies with tree cover: Red-edge position has a strong negative effect on LFM C when tree cover is high, a weak negative effect



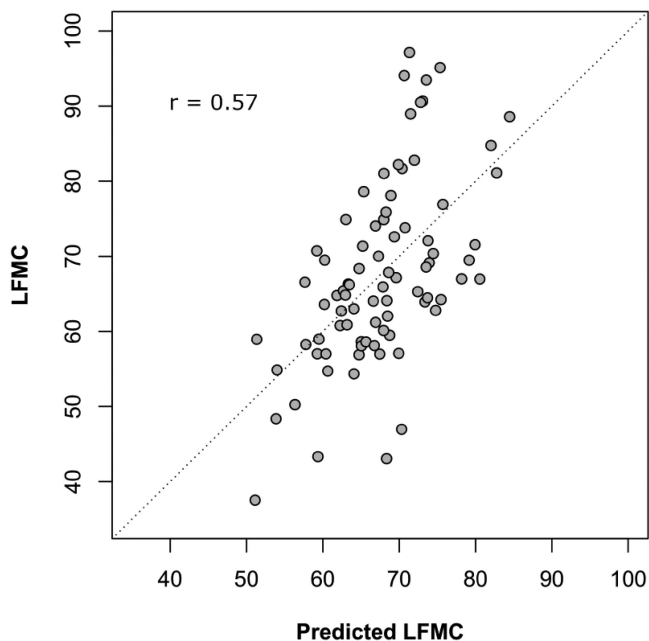


Fig. 3. Relationship between true LFMC (as measured in the field) and LFMC values predicted from the multiple-regression model based on Red-edge position and ancillary data. The dotted line depicts the 1:1 slope. The correlation coefficient between true and predicted LFMC appears in the top left.

when tree cover is intermediate, and a strong positive effect on LFMC when tree cover is very low (Fig. 4).

In contrast to the significant effects of Red-edge position on LFMC, the other vegetation indices failed to yield significant effects on LFMC in models that included ancillary variables about site conditions (see above). Still, the variation in LFMC that was explained by models containing these variables was as high as 25.39% (the model containing red-edge 2 NDVI), followed by 23.64% (NDVI), 23.5% (red-edge 1 NDVI), and 21.81% (CWCI). This nonnegligible amount of variation explained is due to the inherent relationships between timing, slope aspect, tree cover, and LFMC irrespective of the spectral properties of the vegetation in sites.

The effect of each vegetation index on LFMC varied among models that accounted for the nested and repeated-measures structure of our data. Red-edge position, NDVI, and Red-edge 2 NDVI had significant positive effects on LFMC (Red-edge position:  $\beta = 2.01$  (S.E. 0.71),  $p = 0.005$ ; NDVI:  $\beta = 26.17$  (S.E. 12.3),  $p = 0.03$ ; Red-edge 2 NDVI:  $\beta = 152.02$  (S.E. 58.61),  $p = 0.009$ ). Red-edge 1 NDVI had a marginally-significant positive effect on LFMC ( $\beta = 28.15$  (S.E. 15.09),  $p = 0.05$ ), and the effect of CWCI on LFMC was nonsignificant. Analysis of the random effects of these models revealed a considerable variation in LFMC among sites and across plots within sites which was not explained by the VI's.

### C. Comparison With Sentinel 2 Vegetation Indices

Of the six Sentinel 2 vegetation indices that were tested as predictors of LFMC, only two, GVMI and NDII, proved to be

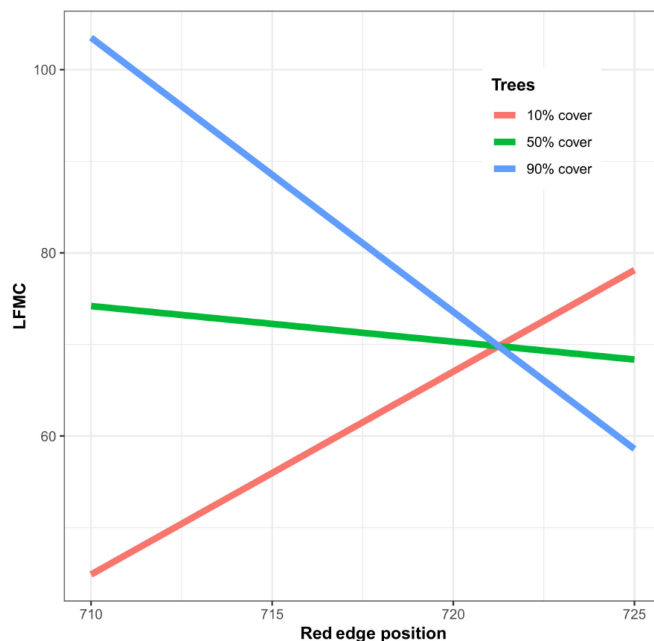


Fig. 4. Interactive effects of Red-edge position and tree cover on LFMC based on the multiple-regression model. Red-edge position switches from a negative effect on LFMC at intermediate to high tree cover to a positive effect on LFMC when tree cover is low.

significant predictors in LFMC models that also contained ancillary data. Both GVMI and NDII contain spectral information from SWIR bands, in contrast to the other four VI's tested in this study (which contained data from visible and near infrared bands only) which were not significant predictors of LFMC. The lack of a significant effect of Sentinel's red-edge position on LFMC contrasts with the significant effect of VEN $\mu$ S's red-edge position index on LFMC. In addition, models containing either GVMI or NDII explained considerably less variation in LFMC ( $\sim 21\%$ ) compared to the model containing VEN $\mu$ S's red-edge position index (32.5%; see previous paragraph).

The model that included NDII, tree cover, the interaction of NDII and tree cover, slope-aspect, and Julian day as predictors of LFMC was statistically significant ( $p < 0.001$ ) and explained 20.9% of the variation in LFMC across sampling sites and dates. According to this model, Julian day had a significant negative effect on LFMC ( $\beta = -0.09$  (S.E. 0.03),  $p = 0.002$ ), yet tree cover and slope-aspect did not have a significant effect on LFMC. NDII had a significant positive effect on LFMC ( $\beta = 53.57$  (S.E. 20.23),  $p = 0.009$ ), and the interaction between NDII and tree cover was significantly negative ( $\beta = -72.03$  (S.E. 36.24),  $p = 0.049$ ). Similarly, a model with the same variable composition in which GVMI replaced NDII as a predictor was significant ( $p < 0.001$ ), and explained 20.6% of the variation in LFMC. Here, too, Julian day had a significant negative effect on LFMC ( $\beta = -0.1$  (S.E. 0.03),  $p = 0.001$ ), tree cover had a significant positive effect ( $\beta = 17.22$  (S.E. 7.39),  $p = 0.02$ ), and northern and southern facing aspects had significantly lower LFMC than flat areas ( $\beta = -5.51$  (S.E. 2.39),  $p = 0.02$ ; and  $\beta = -7.18$  (S.E. 3.15),  $p = 0.02$ , respectively). GVMI had a

significant positive effect on LFMCI ( $\beta = 41.39$  (S.E. 16.76),  $p = 0.01$ ), and the interaction between GVMI and tree cover was significantly negative ( $\beta = -68.67$  (S.E. 28.64),  $p = 0.018$ ). In both NDII and GVMI models, the negative interaction between VI and tree cover implies that the effect of the given VI on LFMCI varies with tree cover: The VI has a moderate negative effect on LFMCI when tree cover is high (90%), a moderate positive effect when tree cover is intermediate (50%), and a strong positive effect on LFMCI when tree cover is very low (10%) (Figures S2 and S3, for NDII and GVMI, respectively). These results are qualitatively the same with those obtained for VEN $\mu$ S's red-edge position index at the 10th and 90th percentiles (whereas at the 50th percentile the direction of the effect is opposite). Given the moderately high correlation among Sentinel's NDII and GVMI (Pearson's  $r = 0.94$ ), the overall similarity between their models is not surprising. Yet the similarity in effect sizes between the NDII and GVMI models and the model containing VEN $\mu$ S's red-edge position index is unexpected, given the correlations between these variables are very low ( $r = 0.19$  and  $r = 0.09$ ; for red-edge position versus GVMI and NDII, respectively).

#### IV. DISCUSSION

In this study we assessed the potential of utilizing high spatial resolution satellite data acquired by VEN $\mu$ S to quantify LFMCI in eastern Mediterranean ecosystems in Israel. Despite the lack of SWIR bands, Red-edge position values extracted from VEN $\mu$ S data, together with ancillary variables, were moderately successful in estimating field-collected LFMCI values. Given the vast variation in climate, soils, topography, and vegetation composition within and among our study sites (which were located along a steep precipitation gradient), the performance of the model was better than expected. Surprisingly, the LFMCI model based on VEN $\mu$ S's Red-edge position index outperformed all models based on Sentinel 2 VI's, despite the latter containing spectral information in the SWIR range. A potential explanation for this performance difference is the high spatial heterogeneity in Mediterranean vegetation, which is better captured by VEN $\mu$ S's 10-m spatial resolution compared to Sentinel's 20-m resolution in the SWIR bands.

The two separate modeling approaches we used to predict LFMCI highlighted the large variation in site and plot conditions, which emphasize the difficulty of using remote sensing to predict LFMCI in eastern Mediterranean ecosystems. In the single-predictor mixed effects models, four out of the five VI had a significant or quasi-significant effect on LFMCI. These models, after all, lump all variation in LFMCI due to difference among sites and plots without revealing their causes (i.e., the random effect), and hence contain the hidden effects of many possible site and plot characteristics that are not captured by any VI. In contrast, in the multiple regression models that included site and plot characteristics as predictor variables (on top of a given VI), only red-edge position proved to be a significant predictor of LFMCI. We suggest that the difference in the results of the two modeling approaches (in terms of VI performance as a predictor of LFMCI) is caused by missing predictors in

the multiple regression models, which may reflect site and plot conditions that affect LFMCI but are not captured by either VI or any of the ancillary predictor variables. One such predictor is a measure of species composition, as LFMCI varies considerably among species, and even within individuals and across time [38]–[40]. Unfortunately, it is impossible to map species identity from remotely sensed data in Mediterranean ecosystems because the spectral variation across individuals of the same species often exceeds the spectral variation among individuals of different species [30], [35]. Consequently, we opted not to include species-level variables as predictors in our multiple regression model of LFMCI, as we wanted to restrict its ancillary variables to those that can be obtained from remote sensing (e.g., tree cover), are readily available from national GIS databases (e.g., slope aspect), or can be derived directly from the data (e.g., Julian date).

The multiple regression model of LFMCI as a function of red-edge position and ancillary variables had a significant interaction term between Red-edge position and tree cover. Qualitatively similar results (i.e., a negative interaction between VI and tree cover) were found in models containing Sentinel's NDII and GVMI. The interaction analysis revealed an unexpected pattern, in which Red-edge position had a strong negative effect on LFMCI when tree cover was high (this itself is unsurprising—as leaves of woody species dry-out, the red edge becomes more gradual and its inflection point should shift to longer wavelengths), but a strong positive effect on LFMCI when tree cover was small. This positive effect is counterintuitive, as it suggests a positive relationship between senescence and LFMCI. At present, we do not have a reasonable explanation to why plots with little tree cover (but that contain shrubs and dwarf-shrubs) exhibit this pattern.

Our general finding about the only-moderate capability of VI's extracted from VEN $\mu$ S (and to even a lesser extent, Sentinel 2 VI's) data to predict LFMCI in eastern Mediterranean ecosystems in Israel raises an important question: Are the predictions of the model based on VEN $\mu$ S data accurate enough to support monitoring and management activities aimed at identifying areas of high wildfire risk due to low LFMCI levels? We suggest that the answer is not clear-cut. At present, the only viable alternatives for mapping LFMCI from satellite data may be based on vegetation indices derived from Sentinel or Landsat data [27], at spatial resolutions of 20–30 m, with a considerably less frequent revisit time compared to VEN $\mu$ S (i.e., several days at best). Yet our results regarding the feasibility of Sentinel 2 data reveal that the predictive ability of its VI's is even weaker than those of VEN $\mu$ S's. Alternatively, MODIS [28] offers daily revisit times, but at a much coarser spatial resolution (500 m) which we deem insufficient to capture LFMCI dynamics in eastern Mediterranean ecosystems because they are characterized by extremely high spatial heterogeneity at fine grains [30], [36]. A promising avenue for overcoming the shortfalls of VEN $\mu$ S for mapping LFMCI (namely, the lack of SWIR bands) may be based on utilizing information on the distinctive phenological patterns of the main vegetation types in Mediterranean ecosystems. This information can support the implementation of deep

learning algorithms, which can combine information derived from long-term time series of VEN $\mu$ S data and coupled with continuous field sampling campaigns to yield continuous estimates of LFMC. At present, a study on the application of deep-learning algorithms for mapping the composition of the main vegetation types in eastern Mediterranean ecosystems using VEN $\mu$ S data is underway, and we hope that its results will facilitate a similar analysis in the context of LFMC.

#### ACKNOWLEDGMENT

The authors would like to thank Eyal Weizmann, Guy Nahardiya, and Ella Fishman for helping in field data collection and lab work. They also thank two reviewers for insightful comments that greatly improved this article.

#### REFERENCES

- [1] Z. Naveh and J. Dan, "The human degradation of Mediterranean landscapes in Israel," in *Mediterranean Type Ecosystems: Origin and Structure*, F. di Castri, H. A. Mooney, Eds. Berlin, Heidelberg: Springer, 1973, pp. 373–390.
- [2] P. W. Rundel, "Landscape disturbance in Mediterranean-Type ecosystems: An Overview," in *Landscape Disturbance and Biodiversity in Mediterranean-Type Ecosystems*, P. W. Rundel, G. Montenegro, and F. M. Jaksic, Eds. Berlin, Heidelberg: Springer, 1998, pp. 3–22.
- [3] T. Plieninger, C. Hui, M. Gaertner, and L. Huntsinger, "The impact of land abandonment on species richness and abundance in the Mediterranean Basin: A Meta-Analysis," *PLOS ONE*, vol. 9, no. 5, May 2014, Art. no. e98355.
- [4] J. G. Pausas and V. R. Vallejo, "The role of fire in European Mediterranean ecosystems," in *Remote Sensing of Large Wildfires in the European Mediterranean Basin*, E. Chuvieco, Ed. Berlin, Heidelberg: Springer, 1999, pp. 3–16.
- [5] N. Levin, N. Tessler, A. Smith, and C. McAlpine, "The human and physical determinants of wildfires and burnt areas in Israel," *Environmental Manage.*, vol. 58, no. 3, pp. 549–562, Sep. 2016.
- [6] M. Turco, N. Levin, N. Tessler, and H. Saaroni, "Recent changes and relations among drought, vegetation and wildfires in the Eastern Mediterranean: The case of Israel," *Global Planet. Change*, vol. 151, pp. 28–35, Apr. 2017.
- [7] A. Perevolotsky and N. G. Seligman, "Role of grazing in Mediterranean rangeland ecosystems," *BioScience*, vol. 48, no. 12, pp. 1007–1017, Dec. 1998.
- [8] D. Bashan and A. Bar-Massada, "Regeneration dynamics of woody vegetation in a Mediterranean landscape under different disturbance-based management treatments," *Appl. Vegetation Sci.*, vol. 20, no. 1, pp. 106–114, Jan. 2017.
- [9] Y. Carmel, S. Paz, F. Jahashan, and M. Shoshany, "Assessing fire risk using Monte Carlo simulations of fire spread," *Forest Ecology Manage.*, vol. 257, no. 1, pp. 370–377, Jan. 2009.
- [10] A. Bar Massada, V. C. Radeloff, S. I. Stewart, and T. J. Hawbaker, "Wildfire risk in the wildland–urban interface: A simulation study in northwestern Wisconsin," *Forest Ecology Manage.*, vol. 258, no. 9, pp. 1990–1999, Oct. 2009.
- [11] S. Paz, Y. Carmel, F. Jahshan, and M. Shoshany, "Post-Fire analysis of pre-fire mapping of fire-risk: A recent case study from Mt. Carmel (Israel)," *Forest Ecology Manage.*, vol. 262, no. 7, pp. 1184–1188, Oct. 2011.
- [12] R. C. Rothermel, "How to predict the spread and intensity of forest and range fires," Intermountain Forest Range Experiment Station, US Dept. Agriculture, Ogden, UT, USA, General Tech. Rep. INT-143, vol. 143, 1983.
- [13] M. P. Plucinski, W. R. Anderson, R. A. Bradstock, and A. M. Gill, "The initiation of fire spread in shrubland fuels recreated in the laboratory," *Int. J. Wildland Fire*, vol. 19, no. 4, pp. 512–520, Jul. 2010.
- [14] L. S. Bradshaw, J. E. Deeming, R. E. Burgan, and J. D. Cohen, "The 1978 national fire-danger rating system: Technical documentation," Intermountain Forest Range Experiment Station, US Dept. Agriculture, Ogden, UT, USA, General Tech. Rep. INT-169, vol. 169, 1984.
- [15] M. A. Finney, "FARSITE: Fire Area Simulator-model development and evaluation," Intermountain Forest Range Experiment Station, US Dept. Agriculture, Ogden, UT, USA, Res. Paper RMRS-RP-4, vol. 4, 1998.
- [16] S. A. J. Anderson and W. R. Anderson, "Ignition and fire spread thresholds in gorse (*Ulex europaeus*)," *Int. J. Wildland Fire*, vol. 19, no. 5, pp. 589–598, Aug. 2010.
- [17] J. E. Keeley, C. J. Fotheringham, and M. A. Moritz, "Lessons from the October 2003. Wildfires in Southern California," *J. Forestry*, vol. 102, no. 7, pp. 26–31, Oct. 2004.
- [18] J. E. Keeley, H. Safford, C. J. Fotheringham, J. Franklin, and M. Moritz, "The 2007 southern California wildfires: Lessons in complexity," *J. Forestry*, vol. 107, no. 6, pp. 287–296, Sep. 2009.
- [19] I. Oliveras, M. Gracia, G. Moré, and J. Retana, "Factors influencing the pattern of fire severities in a large wildfire under extreme meteorological conditions in the Mediterranean basin," *Int. J. Wildland Fire*, vol. 18, no. 7, pp. 755–764, Nov. 2009.
- [20] R. A. Bradstock, J. S. Cohn, A. M. Gill, M. Bedward, and C. Lucas, "Prediction of the probability of large fires in the Sydney region of south-eastern Australia using fire weather," *Int. J. Wildland Fire*, vol. 18, no. 8, pp. 932–943, Jan. 2010.
- [21] N. Gellie, K. Gibos, and K. Johnson, "Relationship between severe landscape dryness and large destructive fires in Victoria," presented at the VI Int. Conf. Forest Fire Res., Coimbra, Portugal, 2010.
- [22] F. P. Schoenberg, R. Peng, Z. Huang, and P. Rundel, "Detection of non-linearities in the dependence of burn area on fuel age and climatic variables," *Int. J. Wildland Fire*, vol. 12, no. 1, pp. 1–6, 2003.
- [23] P. E. Dennison, M. A. Moritz, and R. S. Taylor, "Evaluating predictive models of critical live fuel moisture in the Santa Monica Mountains, California," *Int. J. Wildland Fire*, vol. 17, no. 1, pp. 18–27, Mar. 2008.
- [24] E. Chuvieco, I. González, F. Verdú, I. Aguado, and M. Yebra, "Prediction of fire occurrence from live fuel moisture content measurements in a Mediterranean ecosystem," *Int. J. Wildland Fire*, vol. 18, no. 4, pp. 430–441, Jul. 2009.
- [25] S. Jurdao, E. Chuvieco, and J. M. Arevalillo, "Modelling fire ignition probability from satellite estimates of live fuel moisture content," *Fire Ecology*, vol. 8, no. 1, pp. 77–97, Apr. 2012.
- [26] M. Yebra et al., "A global review of remote sensing of live fuel moisture content for fire danger assessment: Moving towards operational products," *Remote Sens. Environ.*, vol. 136, pp. 455–468, Sep. 2013.
- [27] E. Chuvieco, D. Riaño, I. Aguado, and D. Cocero, "Estimation of fuel moisture content from multitemporal analysis of Landsat Thematic Mapper reflectance data: Applications in fire danger assessment," *Int. J. Remote Sens.*, vol. 23, no. 11, pp. 2145–2162, Jan. 2002.
- [28] D. A. Roberts, P. E. Dennison, S. Peterson, S. Sweeney, and J. Rechel, "Evaluation of airborne visible/infrared imaging spectrometer (AVIRIS) and moderate resolution imaging spectrometer (MODIS) measures of live fuel moisture and fuel condition in a shrubland ecosystem in southern California," *J. Geophys. Res. Biogeosci.*, vol. 111, no. G4, Dec. 2006, Art. no. G04S02.
- [29] P. E. Dennison, D. A. Roberts, S. H. Peterson, and J. Rechel, "Use of normalized difference water index for monitoring live fuel moisture," *Int. J. Remote Sens.*, vol. 26, no. 5, pp. 1035–1042, Mar. 2005.
- [30] M. Shoshany, "Satellite remote sensing of natural Mediterranean vegetation: A review within an ecological context," *Prog. Physical Geography Earth Environ.*, vol. 24, no. 2, pp. 153–178, Jun. 2000.
- [31] P. Ferrier et al., "VEN $\mu$ S (Vegetation and environment monitoring on a new micro satellite)," in *Proc. IEEE Int. Geosci. Remote Sens. Symp.*, Honolulu, HI, USA, Jul. 2010, pp. 3736–3739.
- [32] A. Dick et al., "VEN $\mu$ S commissioning phase: Specificities of radiometric calibration," in *Proc. IEEE Int. Geosci. Remote Sens. Symp.*, Valencia, Spain, Jul. 2018, pp. 4320–4323.
- [33] J. W. Rouse, "Monitoring vegetation systems in the Great Plains with ERTS," Jan. 1974, Accessed: Aug. 11, 2019. [Online]. Available: <https://ntrs.nasa.gov/search.jsp?R=19740022614>
- [34] A. Gitelson, "Remote sensing estimation of crop biophysical characteristics at various scales," in *Hyperspectral Remote Sensing of Vegetation*. Boca Raton, FL, USA: CRC Press, 2011, pp. 329–358.
- [35] I. Herrmann, A. Pimstein, A. Karnieli, Y. Cohen, V. Alchanatis, and D. J. Bonfil, "LAI assessment of wheat and potato crops by VEN $\mu$ S and Sentinel-2 bands," *Remote Sens. Environ.*, vol. 115, no. 8, pp. 2141–2151, Aug. 2011.
- [36] A. Bar Massada, O. Gabay, A. Perevolotsky, and Y. Carmel, "Quantifying the effect of grazing and shrub-clearing on small scale spatial pattern of vegetation," *Landscape Ecology*, vol. 23, no. 3, pp. 327–339, Jan. 2008.



- [37] A. Bar Massada, R. Kent, L. Blank, A. Perevolotsky, L. Hadar, and Y. Carmel, "Automated segmentation of vegetation structure units in a Mediterranean landscape," *Int. J. Remote Sens.*, vol. 33, no. 2, pp. 346–364, Jan. 2012.
- [38] E. W. Pook and A. M. Gill, "Variation of live and dead fine fuel moisture in *Pinus radiata* plantations of the australian-capital-territory," *Int. J. Wildland Fire*, vol. 3, no. 3, pp. 155–168, 1993.
- [39] A. P. Dimitrakopoulos and K. K. Papaioannou, "Flammability assessment of Mediterranean forest fuels," *Fire Technol.*, vol. 37, no. 2, pp. 143–152, Apr. 2001.
- [40] T. H. Fletcher *et al.*, "Effects of moisture on ignition behavior of moist California chaparral and Utah leaves," *Combustion Sci. Technol.*, vol. 179, no. 6, pp. 1183–1203, May 2007.



**Avi Bar-Massada** received the Ph.D. degree in soil, water, and environmental engineering from the Technion – Israel Institute of Technology, Haifa, Israel, in 2008.

From 2009 to 2011 he was a Research Associate with the Department of Forest and Wildlife Ecology, University of Wisconsin–Madison, Madison, WI, USA. Since 2012, he has been a Faculty Member with the Department of Biology and Environment at the University of Haifa–Oranim, in Kiryat Tivon, Israel. He is a Landscape and Spatial Ecologist, with

particular interest in quantifying the effects of spatial patterns of landscapes on the ecological processes within them. His main research interests include understanding the relationship between wildfire and human settlements, the role of anthropogenic disturbances in shaping the patterns of vegetated communities, and the effect of environmental heterogeneity on ecological processes. To study these topics, he uses a variety of scientific tools, including mathematical models, advanced statistical analyses, remote sensing methods (focusing on image classification and segmentation, and analysis of LiDAR data), and geographic information systems.



**Achiad Sviri** received the B.Sc. in biology from the University of Haifa, Haifa, Israel, in 2019. He is currently working toward the M.Sc. degree with the Department of Environmental and Evolutionary Biology at the University of Haifa. His M.Sc. thesis focuses on developing image processing methods for automated taxonomic identification of insects on sticky traps; and to quantify the relationships between the spatial structure of Eucalypt forests and two insect species.

From 2016 to 2018 he worked on mapping and assessing the conservation threat to lizard species along the coastal plain of Israel, where development pressure is rampant. His work focused on the effects of planting Eucalypt (a foreign tree) on a local lizard species which is under extinction threat.